REVIEW

Inhibition of Bacterial RNA Polymerase Function and Protein-Protein Interactions: A Promising Approach for Next-Generation Antibacterial Therapeutics

Received 00th January 20xx,
Accepted 00th January 20xx

DOI: 10.1039/x0xx00000x

Jiqing Ye,†[a,b] Cheuk Hei Kan,†[c] Xiao Yang*[c] and Cong Ma*[a]

The increasing prevalence of multidrug-resistant pathogens necessitates the urgent development of new antimicrobial agents with innovative modes of action for the next generation of antimicrobial therapy. Bacterial transcription has been identified and widely studied as a viable target for antimicrobial development. The main focus of these studies has been the discovery of inhibitors that bind directly to the core enzyme of RNA polymerase (RNAP). Over the past two decades, substantial advancements have been made in understanding the properties of protein-protein interactions (PPIs) and gaining structural insights into bacterial RNAP and its associated factors. This has led to the crucial role of computational methods in aiding the identification of new PPI inhibitors to affect the RNAP function. In this context, bacterial transcriptional PPIs present promising, albeit challenging, targets for the creation of new antimicrobials. This review will succinctly outline the structural foundation of bacterial transcription networks and provide a summary of the known small molecules that target transcription PPIs.

1. Introduction

Bacterial infections have posed significant challenges to human health for centuries, and the discovery of antibiotics revolutionized the field of medicine by providing effective treatments [1]. However, the rapid emergence and spread of antibiotic resistance among bacterial pathogens have compromised the efficacy of these life-saving drugs [2-4]. Therefore, developing new antibacterial therapeutics with novel mechanisms of action is crucial to addressing the ongoing antibiotic resistance crisis.

RNA plays a crucial role in the life cycles of organisms across the three domains of life, and its synthesis is referred to as transcription [5]. Generally, RNA is synthesized using DNA as a template, resulting in the production of different types of RNA molecules, such as messenger RNA (mRNA), transfer RNA (tRNA), and ribosomal RNA (rRNA) [6]. These RNA molecules are then utilized in translation, in which proteins are synthesized in a mRNA-dependent manner [7, 8]. Notably, some RNA viruses use their RNA genome as a template to synthesize mRNA or make an complementary DNA (cDNA) molecule from the RNA (reverse transcription), subsequently using it to advance their life circle in host cells [9, 10].

Bacterial transcription is an attractive target for the development of antibacterial agents [11, 12]. Generally, there are two strategies targeting bacterial transcription. The first involves the direct inhibition of subunits within RNA polymerase (RNAP), while the second is the disruption of the contacts between transcription factors and RNAP core or other factors. Over the past decades, various classes of antibacterial agents have been developed to bind to different sites on bacterial RNAP, including clinically available compounds rifamycin and lipiarmycin [13, 14]. In recent years, significant progress has been made in elucidating the structures and functions of transcription factors and their contacts with RNAP and other factors. Of note, the identification of critical residues, often referred to as “hotspots”, has facilitated the discovery of protein-protein interaction (PPI) inhibitors with potent antimicrobial activity.

Previously, Ma *et al.* reviewed the bacterial transcription and inhibitors that bind to different sites on RNAP [11]. More recently, the development of modulators of bacterial PPIs and natural products as antimicrobial agents are summarized [15, 16]. In this perspective, we aim to present the current status of research on bacterial RNAP and transcription factors, especially those that have the potential to be targets for the development of next-generation antibacterial therapeutics. We will emphasize the inhibitors that have been identified thus far and discuss the methods used to screen the hit compounds and their subsequent optimization process.

[a] *State Key Laboratory of Chemical Biology and Drug Discovery, Department of Applied Biology and Chemical Technology, The Hong Kong Polytechnic University, Kowloon, Hong Kong SAR, China.*
[b] *School of Pharmacy, Inflammation and Immune Mediated Diseases Laboratory of Anhui Province, Anhui Medical University, Hefei 230032, China.*
[c] *Department of Microbiology, The Chinese University of Hong Kong, Prince of Wales Hospital, Shatin, Hong Kong SAR, China*
** Correspondances: conq.ma@polyu.edu.hk; xiaoyang@cuhk.edu.hk*
† Jiqing Ye and Cheuk Hei Kan contributed equally to this work.

2. RNA polymerase and clinically used inhibitors

2.1. RNA polymerase

In all three domains of life, multi-subunit RNAPs are the primary enzymes responsible for catalyzing the synthesis of RNA from a DNA template during transcription. Bacteria and archaea utilize only one type of RNAP to transcribe all their genes, whereas eukaryotes utilize four different types of RNAPs (RNAP I, II, III and IV) that transcribe specific subsets of genes without overlapping [17]. Amongst, RNAP II is specifically responsible for the synthesis of mRNA.

It becomes increasingly clear that all RNAPs are derived from a common ancestor, as evidenced by their amino acid sequence, subunit composition, structures, functions, and molecular mechanisms [18, 19]. Moreover, the subunit arrangement of all RNAPs shares a common architecture consisting of five subunits, which form the universally conserved core of the RNAP [20]. This core structure, which primarily represents the modern bacterial RNAP, accounts for about 75% of the protein mass in archaeal and eukaryotic RNAPs (**Fig. 1**) [21].

Bacterial RNAP is the simplest form of RNAP found among the three domains of life and exists in two forms: the core enzyme and holoenzyme. The core enzyme consists of five subunits: α-dimer (α_2), β, β' and ω [18]. The binding of a single protein, the initiation factor σ, to the core enzyme results in the formation of a holoenzyme, which is the active form of RNAP that is essential for transcription initiation [22].

Eukaryotic RNAP II, on the other hand, are composed of Rpb1 to Rpb12 subunits, with the numbering based on the subunits in *Saccharomyces cerevisiae*, whereas the archaeal RNAP subunits are named Rpo1 to Rpo13 [23]. It is noteworthy that, although archaea and bacteria are both prokaryotes, at the molecular level, archaea RNAP is much more closely related to eukaryotes than bacteria. [24] This relationship is supported by molecular characterization and further reinforces the division between the bacterial and archaeal-eukaryotic branches of the universal tree of life. Notably, one of the structural evidence is the presence of a stalk-like protrusion in the core of archaeal and eukaryotic RNAP at a right angle to the transcription direction, which is absent in bacterial RNAP (**Fig. 1**) [25].

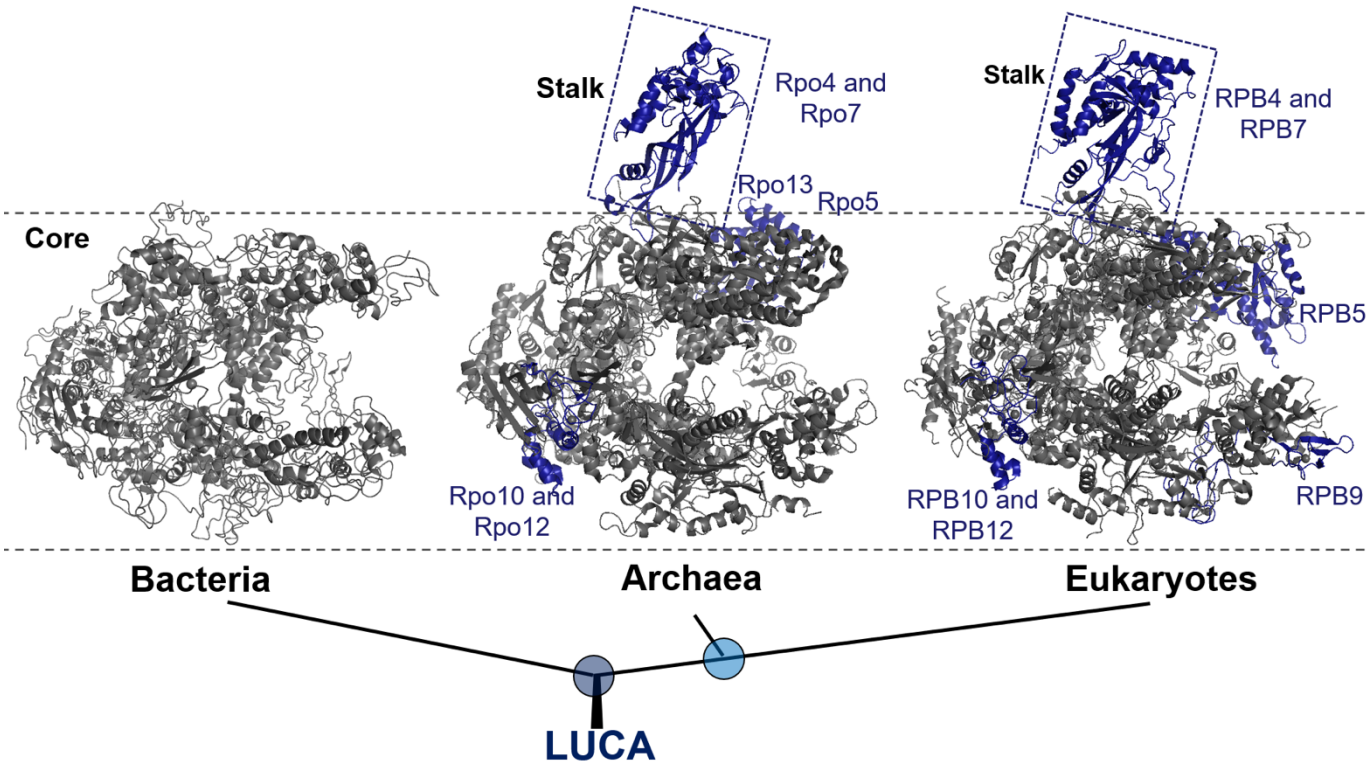

Fig. 1 Evolution of RNAP structures in the three domains of life from the last universal common ancestor (LUCA). Bacteria: *Thermus aquaticus* (PDB 1I6V); Archaea: *Saccharolobus shibatae* (PDB 2WAQ); Eukaryotes: *Saccharomyces cerevisiae* RNAP II (PDB 1Y1W). Universally conserved RNAP core subunits are denoted in gray, while subunits unique to the archaeal-eukaryotic lineage are labeled and colored density blue.

Structural studies of bacterial RNAP date back to the mid-1960s, and the crystallization of RNAP isolated from *Thermus thermophilus* was first reported in the late 1970s [26]. In 1999, Darst *et al.* described the X-ray crystal structure of bacterial RNAP core enzyme (PDB 1HQM) (**Fig. 2**), which was isolated from *T. aquaticus* [26, 27]. The core enzyme exhibits a crab claw shape, with a central active site and pincers that bind DNA between them [28]. One arm of the claw is primarily the β subunit, and the other is primarily the β' subunit. The assembly of the β and β' subunits is aided by the dimer of the α subunit N-terminal

domain (αNTD), and the ω subunit completely wraps around the C-terminal tail of β' subunit [27, 28].

Studies have shown that the active sites of RNAPs are highly conserved across the three domains of life. These active sites are located in the cleft formed by the largest RNAP subunits, β/β' in Bacteria, Rpb1/Rpb2 in Eukarya, and Rpo1/Rpo2 in Archaea [29, 30]. In the vicinity of the active site, the α-helical "bridge" (bridge helix, BH) connects the β and β' clamps, and the two flexible α-helices form a "trigger" loop (TL). In addition to the active site, the cleft contains the primary, secondary, and RNA exit channels (**Fig. 2**). These structural features form the structural basis for the functions of RNAP [26].

During bacterial transcription, the RNAP utilizes several channels to facilitate the process. The primary channel accommodates the double-stranded DNA (dsDNA) template and guides it into the active center cleft of the RNAP. The switch region facilitates conformational changes of the RNAP enzyme, enabling the proper loading of DNA into the active center cleft. Meanwhile, nucleoside triphosphates (NTPs) enter the active center through the secondary channel, serving as building blocks for RNA synthesis. As transcription proceeds, the RNA/DNA hybrid strand is threaded through the active center, and the RNA chain is extruded through the RNA exit channel [31]. These channels, hence, play essential roles in the progression of bacterial transcription by facilitating the movement of DNA, NTPs, and the synthesized RNA within the RNAP complex.

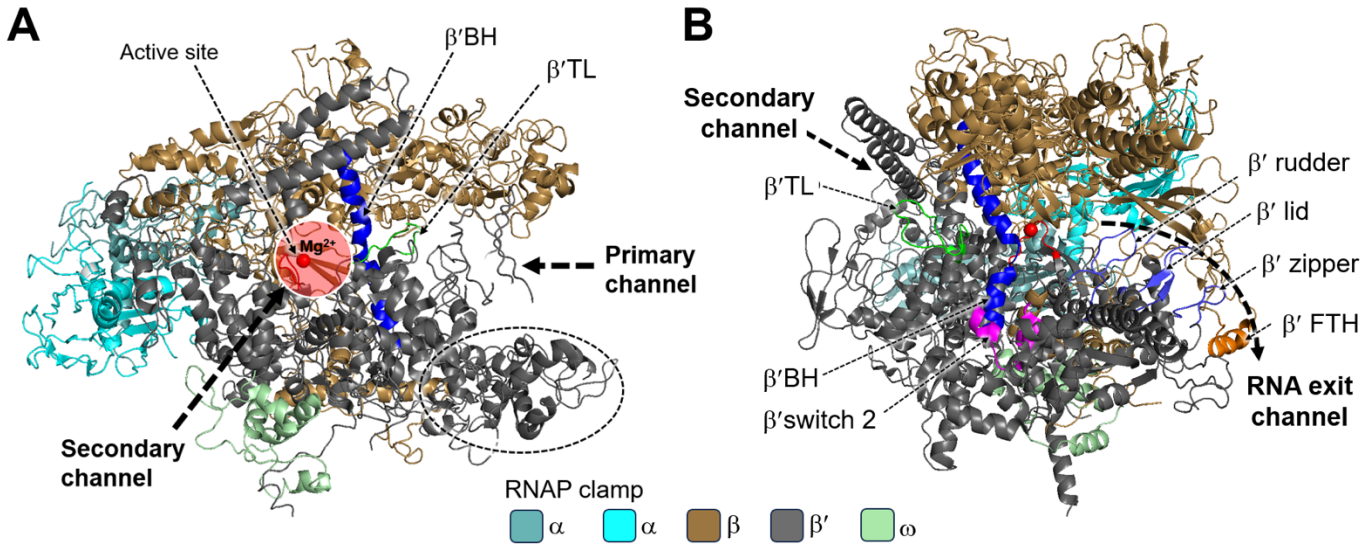

Fig. 2 Structural overview of RNAP core and functional motifs from *T. aquaticus* (PDB 1HQM). **A)** Secondary channel view; **B)** Primary channel view. The structure is represented as colored ribbons with important domains and structural elements indicated. The directions of primary, secondary and RNA exit channels are indicated by black dashed arrows.

2.2. Inhibitors binding to bacterial RNAP directly

RNAP is an essential enzyme for the viability of organisms and has consequently become a proven target for antibacterial [11, 16, 32], anticancer [33] and antiviral [34, 35] drug discovery. In the context of bacteria, RNAP is a critical enzyme for gene expression, making it an attractive target for antibacterial therapies. Moreover, RNAP is highly conserved in a wide range of bacterial species, providing a basis for broad-spectrum activity. Together with its low conservation characteristic in eukaryotic RNAPs, which offers a basis for therapeutic selectivity, RNAP is a promising target for antibacterial drug development [36].

Currently, bacterial RNAP is the target of two classes of antibacterial drugs in clinical use: rifamycin and lipiarmycin (fidaxomicin) [22]. In addition, several other bacterial RNAP inhibitory agents have been reported, including sorangicin and GE23077 as primary channel inhibitors, streptolydigin, salinamide and CBR703 as inhibitors targeting the mobile element of the primary channel, tagetitoxin and microcin J25 as secondary channel inhibitors, and myxopyronins and squaramides as switch region inhibitors [11, 16]. The binding sites of these inhibitors are illustrated in **Fig. 3**. However, despite their potential, none of them enter clinical use as antimicrobials. This is mainly due to their binding sites being located at or near the active site of RNAP, making the

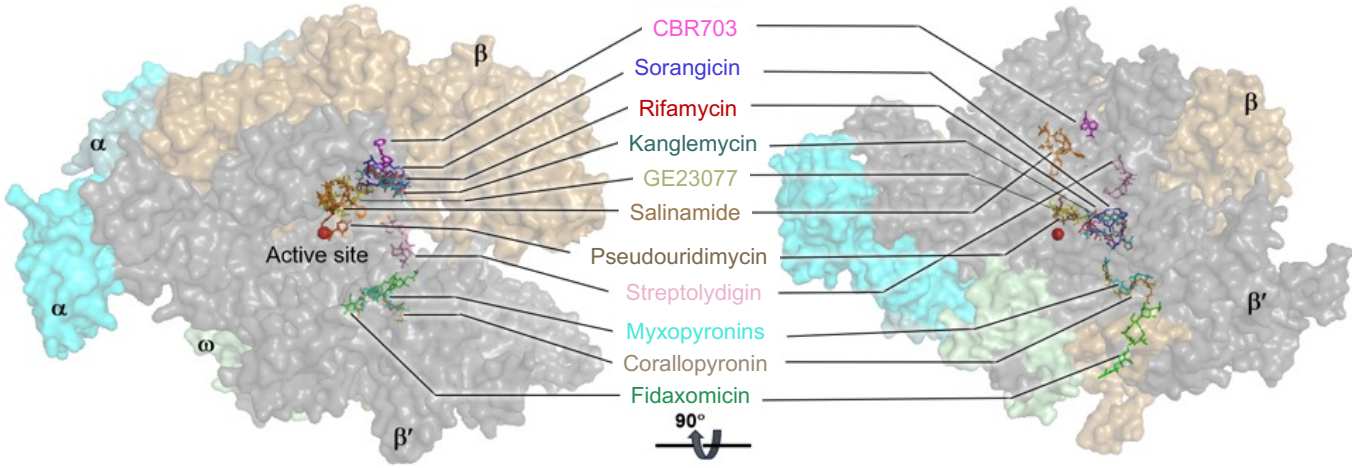

Fig. 3 RNAP inhibitors and their corresponding binding sites.

development of resistance through point mutations more likely. In addition, most of the molecules are natural products with complex structures which are difficult to prepare [11].

Rifampicin. Rifampicin is one of the most successful antibiotics introduced in the 1960s and remains a first-line drug for the treatment of tuberculosis. In the crystal structure of *T. aquaticus* RNAP core complexed with rifampicin, it has been observed that rifampicin binds to a pocket within the β subunit of RNAP, located in the main RNA/DNA hybrid channel with more than 12 Å away from the active site of RNAP (**Fig. 4**) [37]. Bacteria become resistant to rifampicin mainly through mutations in the residues of the binding pocket, as well as through other mechanisms, such as duplication of the target, the action of RNAP-binding proteins, modification of rifampicin itself, and alteration of cell permeability [38].

Lipiarmycin. Unlike rifampin, lipiarmycin preferentially inhibits holoenzyme transcription at a much greater rate than the transcription of the core enzyme [39]. Lipiarmycin targets the σ^{70} (in *Escherichia coli*) subunit region 3.2 and the RNAP β' subunit switch-2 element, which controls the clamping of promoter DNA within the RNAP active-site cleft. Upon binding, the isomerization of the closed-to-open promoter complex is disrupted [40]. The Cryo-electron microscopy (Cryo-EM) structure of *Mycobacterium tuberculosis* RNAP holoenzyme in complex with fidaxomicin at 3.5 Å resolution demonstrated that the binding site of fidaxomicin on RNAP does not overlap with the binding sites of other RNAP inhibitors, including rifampicin (**Fig. 3** & **4**) [41].

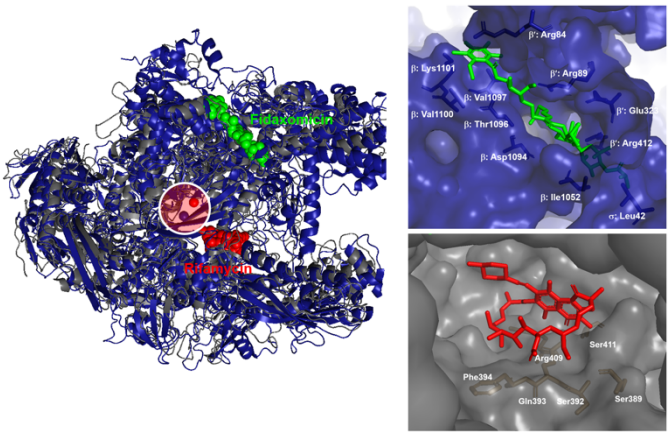

Fig. 4 X-ray structure of rifamycin in complex with RNAP (gray, PDB 1I6V) and Cryo-EM structure of fidaxomicin in complex with RNAP (density blue, PDB 6FBV). Rifamycin and fidaxomicin are colored red and green, respectively.

3. Bacterial transcription cycle

During the past few years, exciting progress has been made in understanding the bacterial transcription cycle, especially through the application of single-molecule techniques. These techniques enable us to visualize the real-time movements of RNAP on the DNA template, providing a wealth of quantitative and direct information about transcriptional structures and dynamics [42, 43]. In general, the transcription cycle can be divided into three phases: initiation, elongation, and termination. While the RNAPs and general transcription cycle are conserved across the three domains of life, details of the regulators in each phase of the cycle can differ among and within different domains of life. In bacteria, the evolution of transcription factors is a good example of this.

To ensure transcription in a temporally and spatially coordinated manner during cell growth and development, the enzymatic activity of bacterial RNAP is tightly regulated by a host of transcription factors throughout all stages of the transcription cycle (**Fig. 5**) [44]. These factors interact with RNAP through PPIs and directly modify its properties at different stages of transcription. Therefore, these factors and their binding sites on RNAP represent potential targets for developing novel drugs.

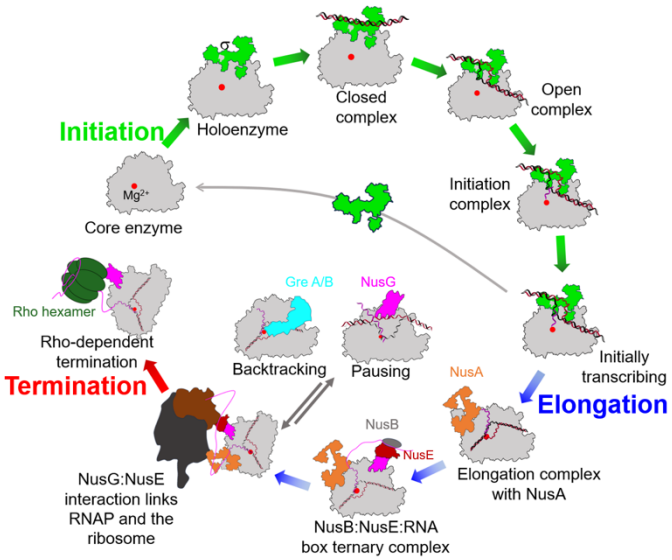

Fig. 5 The bacterial transcription cycle. The process contains three general phases: initiation, elongation, and termination. Some of the critical complexes assembled by RNAP and different transcription factors are illustrated.

3.1. Transcription initiation

In bacteria, transcription initiation is a crucial regulatory step in gene expression regulated by σ factors [45]. Although the RNAP core is competent for RNA polymerization, it requires a σ factor for promoter recognition and opening [46]. Under normal growth conditions, all bacteria possess a primary housekeeping σ factor (such as σ^{70} in Gram-negative bacteria and σ_A in Gram-positive bacteria) that controls the transcription of essential genes [47]. Furthermore, the σ^{70} family of sigma factors is further divided into four major groups. Group 1 comprises the primary σ factor, such as σ^{70} in *E. coli*. Groups 2 to 4 comprise alternative σ factors that play crucial roles in regulating the expression of specific regulons under stress conditions. These alternative σ factors competitively bind to the core RNAP, thereby directing it to specific promoters and regulating the transcription of genes associated with stress responses or specialized functions [48].

Progress in structural biochemistry enables the visualization of the structure of σ factor and its interactions with the RNAP core enzyme. The primary σ factor is composed of four conserved regions: σ regions 1.1, 1.2 to 2.4, 3.0 to 3.2, and 4.1 to 4.2, that constitute four domains $\sigma_{1.1}$, σ_2, σ_3 and σ_4, respectively, along with a non-conserved region (σNCR) (**Fig. 6A**). Crystal structures of the RNAP holoenzyme show that the two amino-terminal domains of the σ subunit (σ_2) interact with β' clamp helices (β'CH), while σ_4 interacts with β-flap-tip-helix (β-FTH) region of RNAP core, forming a V-shaped structure near the opening of the upstream DNA-binding channel of the active site cleft (**Fig. 6A**) [49]. During the core-to-holoenzyme conversion, structural changes of both the core enzyme and the σ factor occur in all the domains of life to facilitate DNA engagement [49]. Subsequently, σ^{70} recognizes the promoter DNA around the -35 and -10 elements to form an open promoter complex through the unwinding of the DNA double helix between the -10 element and the transcription start site (**Fig. 6B**) [50]. Although σ forms extensive contacts with the RNAP core, the most conserved interactions exist between $\sigma_{2.2}$ and the β'CH region [51].

3.2. Transcription elongation

Upon RNAP binding to the promoter, it melts the dsDNA and starts the polymerization of NTPs to produce an RNA molecule. The initial RNA transcript is typically 13 to 15 nucleotides in

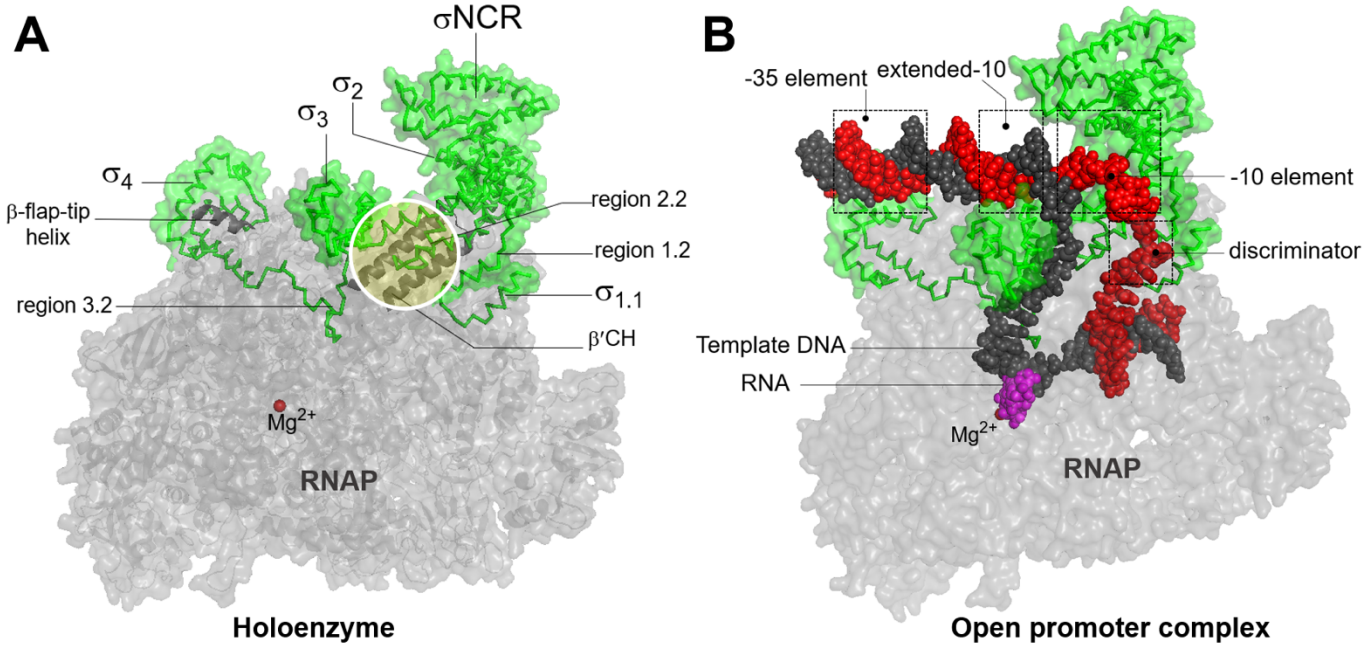

Fig. 6 A) Bacterial RNAP holoenzyme and structural domains and functional motifs of σ factor. $\sigma_{2.2}$ interacts with β'CH and σ_4 interacts with β-β-FTH. **B)** The recognition of housekeeping promoter by holoenzyme forms an open promoter complex. σ4 interacts with the discriminator region. σ factor, non-template DNA (ntDNA), template DNA (tDNA), RNA and are colored green, red, black, magenta. Images are generated using PDB file 4LYN.

length, with 7 to 9 nucleotides forming a pairing with the DNA template strand [52]. Subsequently, the initiation complex undergoes promoter clearance and transition into the elongation complex. The elongation phase of transcription can be divided into two distinct phases: active translocation and pausing [53]. During active translocation, the polymerase incorporates nucleotides into the growing RNA chain and moves forward along the DNA template [54]. In contrast, the paused states represent off-pathway events in the NTP incorporation cycle [55]. In these paused states, the polymerase can either remain stationary at a specific position on the DNA or diffuse backwards along the DNA before recovering from the pause. Throughout the elongation phase, diverse factors interact with the polymerase in both the on-pathway (active translocation) and off-pathway (pausing) phases, thereby modulating either the polymerase's activity or its propensity to enter or remain paused. In *E. coli*, these factors include N-utilizing substance (Nus) factors, RfaH, ribosomal protein S4, Gre-factors (GreA, GreB), Mfd, and RapA (HepA) [44].

NusA. NusA is a critical transcription factor that associates with RNAP and decreases the overall velocity of the process by increasing the pause frequency without affecting the duration of pauses [56]. It binds to the RNAP core after the release of the σ factor and interacts directly with the α, β, β' and the nascent RNA [57].

The crystal structure of NusA, isolated from *M. tuberculosis* (PDB 1K0R), shows that NusA is a multidomain protein consisting of an N-terminal domain (NTD) linked with C-terminal modules which have three RNA binding domains: one S1-like domain and two K homology domains (KH1 and KH2) [58] (**Fig. 7A**). Additionally, certain bacterial species, such as *E. coli*, possess two acidic repeats (AR1, AR2) at the C-terminus of NusA. AR2 contacts with the C-terminal domain (CTD) of the RNAP α subunit (α-CTD), dissociating an auto-inhibitory interaction between AR2 and KH1 and facilitating the binding of RNA to NusA [59]. The Cryo-EM structure of the *E. coli* NusA-RNAP complex (PDB 6FLQ) reveals specific contact points between NusA and paused state at histidine pause site (*his*PEC). These contact points include: i) RNAP α1-CTD with NusA-AR2, ii) RNAP α2-CTD with NusA-NTD, iii) RNAP ω subunit with NusA-KH1/KH2, and iv) RNAP β-FTH with NusA-NTD [60] (**Fig. 7B**). The S1, KH1, and KH2 domains of NusA are integrated together to form an extensive RNA-binding structure [58], while the NusA-NTD interacts with the β-flap region of the RNA exit channel of RNAP [61]. In addition, research has demonstrated that residues F59, R61, E94, and Q96 of the NusA NTD are required for its interaction with conserved residues L895, E899, K900, R903, and E908 in the β-FTH region of RNAP [62].

NusG. NusG is an essential transcription factor, and is also the only universally conserved elongation factor across the three domains of life. Its homologous protein in archaea and eukaryotes is known as Spt5 [63]. NusG interacts with different partners and thereof exerts diverse, or even opposite, functions in the regulation of gene expression. However, its core role is to enhance transcription elongation and RNAP processivity [64]. In *E. coli*, single-molecule assays have shown that the presence of NusG increases the pause-free velocity of RNAP by 10-20% while decreasing the frequency of pauses [65]. This suggests that NusG facilitates efficient transcription elongation by reducing the frequency of pauses in *E. coli*. In contrast, NusG stimulates RNAP pausing by interacting with hairpin-dependent pause sites in the ntDNA strand in *Bacillus subtilis* [66].

NusG is a two-domain protein consisting of the NusG N-terminal domain ($NusG_N$), which binds to RNAP to regulate transcription

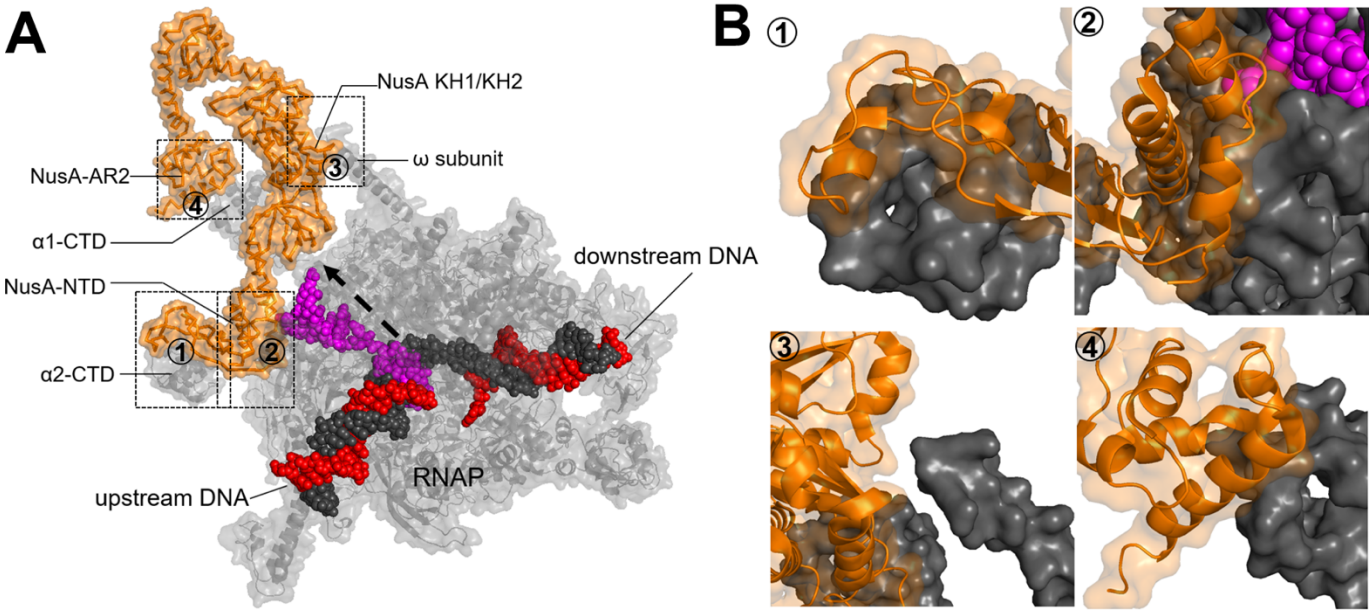

Fig. 7 A) Crystal structure of NusA isolated from *M. tuberculosis* (PDB 1K0R). **B)** Surface representation of *his*PEC-NusA complex. RNAP α1 subunit, α2 subunit, ω subunit, β-flap-tip-helix, NusA, RNA hairpin and upstream and downstream DNA are indicated. The four interaction points are ①RNAP α1-CTD with NusA-AR2; ②RNAP α2-CTD with NusA-NTD; ③RNAP ω subunit with NusA KH1/KH2; ④RNAP FTH with NusA-NTD (PDB 6FLQ).

rates, and the C-terminal ($NusG_C$) Kypride-Onzonis-Woese (KOW) motif, which recruits Rho for termination and NusE (S10) to link transcription and translation [67]. Although a previous biochemical study demonstrated that NusG binds to RNAP weakly without nucleic acids, the crystal structure of the $NusG_N$-RNAP complex from *E. coli* (PDB 5TBZ) [67] was assembled in the absence of nucleic acids. This structure reveals that NusG binds to the central cleft of RNAP, which is surrounded by the β'CH, the protrusion, and the lobe domains (**Fig. 8A**) [67]. When superimposed on the structure of the σ^S-transcription initiation complex, $NusG_N$ is observed to bind at the upstream fork junction, a position similar to σ_2, which may stabilize the upstream junction and thus enhance transcription elongation and RNAP processivity (**Fig. 8B**) [67].

In contrast, NusG stimulates transcription pausing in Gram-positive bacteria like *B. subtilis* by identifying a conserved pause-inducing motif, $_{-11}$TTNTTT$_{-6}$, located on the ntDNA strand within the transcription bubble [66, 68]. Structures of *B. subtilis* NusG and *M. tuberculosis* RNAP have been assembled to investigate the structural basis of NusG-dependent pausing [69]. In the paused transcription complex (PTC), a specific interaction between NusG and ntDNA strand is observed (**Fig. 8C**). However, in the transcription elongation complex (TEC), the

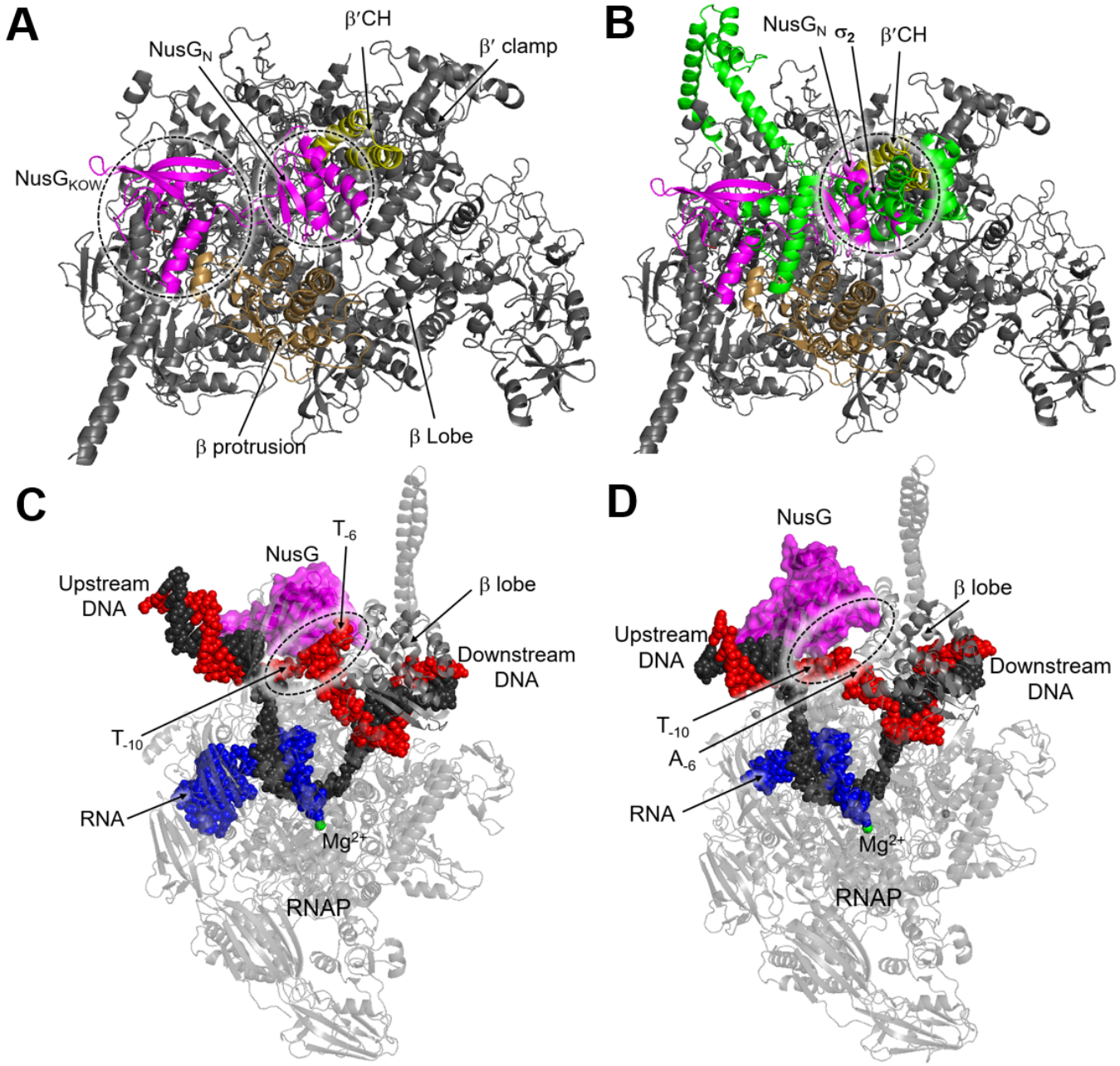

Fig. 8 A) Overall structure of the *E. coli* RNAP-NusG complex (PDB 5TBZ). **B)** Superimposition of the RNAP-NusG with *E. coli* σ^S-transcription initiation complex (PDB 5IPL) via the RNAP. **C)** Cryo-EM structure of NusG-dependent pausing-transcription complex (PTC) assembled by *B. subtilis* NusG and *M. tuberculosis* RNAP (PDB 8EHQ). **D)** Cryo-EM structure of *M. tuberculosis* RNAP elongation complex with *B. subtilis* NusG (PDB 8EOT). RNAP, NusG, σ^S, tDNA, ntDNA and RNA are colored gray, magenta, green, black, red and blue, respectively.

ntDNA passes NusG and RNAP β-lobe domain without any interaction (**Fig. 9D**). The NusG-ntDNA interaction induces rearrangement of the transcription bubble, inhibiting the folding of the TL and allosterically affecting RNA synthesis [69].

NusB. NusB is a protein involved in both transcription and translation processes. This factor, along with NusE and RNA *boxA* sequence, assemble the NusB-NusE-*box*A RNA complex for λ N-mediated antitermination [70, 71]. The solution structure of NusB from *E. coli* was determined by NMR spectroscopy (PDB 1EY1), showing that NusB could be divided into two subdomains. The N-terminal subdomain is formed by helices α1 to α3, while the C-terminal subdomain is formed by helices α4 to α7 [72]. The overall structure of *E. coli* NusB resembles the *M. tuberculosis* NusB protein determined by X-ray diffraction (PDB 1EYV), while the sequence alignment of NusB from *E. coli* and *M. tuberculosis* shows that the amino acid sequences are 57% homologous and 34% identical [72, 73].

NusE. NusE, also known as ribosomal protein S10, is a component of the 30S ribosomal subunit. It interacts with NusB to improve the affinity of the *boxA* RNA to the complex, thus stabilizing the NusB-NusE-RNA ternary complex [74]. The structure of NusE displays the presence of two α-helices (residues 13 to 30, 80 to 87), two β-sheet (residues 5 to 9 and 95 to 99), and a large ribosomal binding loop consisting of residues 43 to 69 [75]. $S10^{\Delta loop}$ mutant study has indicated that the ribosomal binding loop in *E. coli* is dispensable for the transcriptional functions of NusE [76]. An NMR study has further identified the binding sites of NusE on NusB, which involves residues 63 to 81 and 18 to 23 [77]. The crystal structure of the NusB-$S10^{\Delta loop}$ complex (PDB 3D3B) (**Fig. 9A**) displays that NusB and $S10^{\Delta loop}$ approach each other via complementary electrostatic surfaces, and the interfaces between them involve a mixture of hydrophobic and hydrophilic interactions (**Fig. 9A**) [76].

In addition to its contact with NusB, NusE also binds to the $NusG_C$ to anchor the NusB-NusE-*box*A RNA complex to RNAP [78]. The interaction between $NusG_C$ and NusE has been identified through an NMR study (PDB 2KVQ) (**Fig. 9B**). The structure demonstrates that NusE engages L1 and L2 loops on $NusG_c$, which are also involved in binding to the Rho factor during Rho-dependent termination [79]. The competition between NusE and Rho for binding to $NusG_c$ provides a plausible explanation for the inability of Rho to terminate transcription, ensuring the stability of the NusB-NusE-*box*A RNA complex and preventing premature transcription termination mediated by Rho.

Gre factors. The prokaryotic elongation factors Gre factors, for example, GreA in most bacteria and both GreA and GreB in *E. coli*, are reported to enhance the transcription rates of RNAP by suppressing pausing events and inducing RNA cleavage through binding within the secondary channel of RNAP upon backtracking [80]. During this process, RNAP undergoes a reverse sliding motion along the DNA, dissociating the 3' end of the newly synthesized RNA from the template DNA strand, and

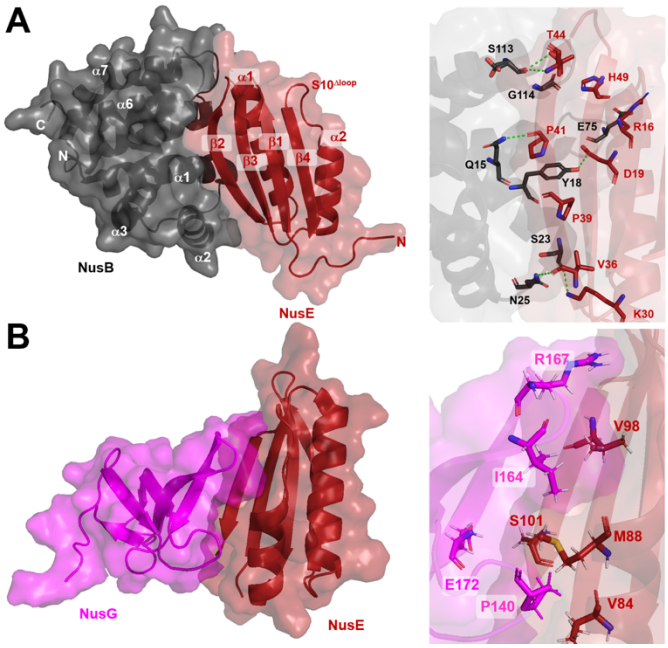

Fig. 9 A) Crystal structure of NusB-$S10^{\Delta loop}$ complex (PDB 3D3B) and details of the interactions between NusB and NusE. **B)** Crystal structure of NusE-$NusG_c$ complex and details of the interactions (PDB 2KVQ).

extruding it into the secondary channel of RNAP [81]. GreA and GreB promote an internal hydrolytic cleavage of the RNA within the backtracked complex catalyzed by the active center of RNAP [82]. The cleavage event enables the continuation of RNA synthesis from the processed end, thereby overcoming the pausing and facilitating transcription elongation. Similar functions to prokaryotic Gre factors are performed by TFIIS in eukaryotic RNAP II and archaeal RNAP [83]. However, there is no structural or sequence similarity between prokaryotic Gre factors and eukaryotic TFIIS [84].

Structurally, both GreA and GreB share a comparable arrangement comprising an coiled-coil NTD and a globular CTD [85, 86]. The NTD is responsible for readthrough and cleavage stimulatory activities, while the CTD contributes to high-affinity binding with the core of RNAP. Despite their similar architectures, there are notable differences in the activities of the two factors [87, 88]. GreB exhibits a significantly higher binding affinity to RNAP, approximately 100-fold tighter than that of GreA. Additionally, while GreA only induces cleavage of only 2 to 3 nucleotides of backtracked RNA, GreB is capable of cleaving RNA fragments up to 18 nucleotides. Upon backtracking, RNAP undergoes conformational changes to form a backtracking complex (BC) that allows a Gre factor to access the active site of RNAP. In *E. coli*, the pre-cleavage complex (PDB 6RIN) of RNAP-GreB reveals that the NTD of GreB extends directly to the active site through the secondary channel of RNAP (**Fig. 10A**) [84]. Consequently, two acidic residues located at the tip of the NTD, namely D41 and E44, are positioned in close proximity to the catalytic site of RNAP (**Fig. 10B**). Outside the RNAP active site channel, the GreB-CTD interacts exclusively with two α helices from the β' that form a part of the entrance rim of the secondary channel [84]. This interaction is critical for the binding

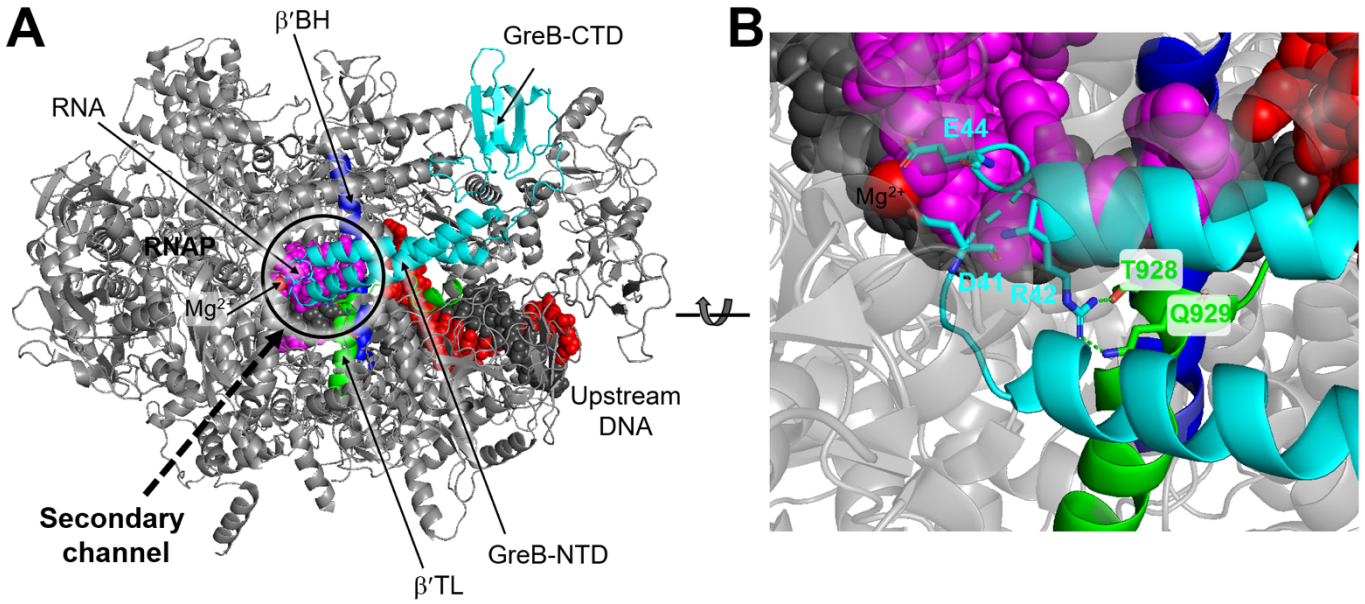

Fig. 10 A) Cryo-EM structure of *E. coli* RNAP backtracked elongation complex bound to GreB transcription factor (PDB 6RIN). **B)** A closed view of GreB-NTD engaged in RNAP active site. GreB, β′ BH and β′ TL, tDNA, ntDNA and RNA are colored cyan, blue, green, black, red and magenta, respectively.

of GreB to RNAP. In particular, two residues within this domain, Asp121 and Pro123, have been identified as crucial for the binding affinity of GreB to RNAP through alanine scanning experiment [89].

3.3. Transcription termination

Transcription termination is a critical process that ensures accurate transcription of the DNA and allows for the recycling of RNAP at the end of transcription. Generally, RNAP undergoes programmed transcription termination through two distinct pathways: factor-independent (intrinsic) and factor-dependent termination. Intrinsic termination in bacteria relies on the core enzymatic activity of RNAP and the presence of a terminal uridine-rich segment on the template DNA chain [90]. Biochemical and single-molecule studies have provided insights into the sequential intermediate states of intrinsic termination. Initially, RNAP halts at the terminator (referred to as the "pause state"). Afterwards, the nascent RNA forms a partial RNA hairpin structure known as the "hairpin-nucleation state" within RNAP. Finally, the RNA hairpin fully folds in the "hairpin-completion state", leading to the dissociation of the RNA from the template DNA strand [91]. Factor-dependent termination, on the other hand, requires specific termination factors that are critical for genomic stability and RNAP recycling [92]. In *E. coli* there are mainly two distinct termination factors, including Rho and Mfd [93].

Rho factor. Rho belongs to the RecA superfamily of ATPases and is a close homolog of F_1-ATPase [94]. Rho-dependent termination is a process where the Rho factor plays a key role. It begins with Rho binding to specific sequences called Rho utilization (rut) sequences on the nascent RNA using its primary binding site (PBS) in an open-ring state. Then, it recognizes a short pyrimidine-rich RNA sequence using its secondary binding site (SBS), which triggers a conformational change into the active state in a closed-ring form. Once in the active state, Rho moves along the RNA molecule in the 5' to 3' direction, with the consumption of ATP in the process, leading to the disruption of the TEC. The Rho-dependent termination process is generally modulated by two elongation factors, NusA and NusG [95]. NusA helps keep Rho in the open-ring state to maintain the transcription elongation, while NusG activates Rho by facilitating the isomerization of the helicase from an open-ring to a closed-ring state [96, 97].

Recently, several structures of the Rho-NusG and Rho-TEC complexes have been reported, providing insights into the molecular interactions involved in the Rho-dependent termination [97-100]. One such structure is the pre-termination complex (PTC) assembled by the elongation complex (EC), NusA, NusG and Rho (PDB 6XAV). In this complex, the Rho hexamer interacts with RNAP subunits in an open-ring conformation, and several critical interfaces between Rho and RNAP are determined [99]. The structure of the PTC displays that NusG bridges RNAP and Rho factor using its NTD and CTD, while NusA stabilizes PTC and directs the nascent RNA into the central channel of Rho hexamer. This arrangement facilitates the interactions between the components of the complex (**Fig. 11A**). Also, structures of functional Rho-dependent PTCs with the Rho hexamer in a closed-ring state have been reported [100]. In these structures, the Rho hexamer is positioned at the opening of the RNA exit channel of RNAP for direct passage of the RNA from the TEC into and through the Rho hexamer, enabling the uridine-rich SBS ligand to bind to Rho SBS site. On the other hand, a trans-supplied RNA oligomer acts as the PBS ligand and interacts with the Rho PBS site (PDB 8E6X, 8E6V) [100]. This complex reveals that Rho monomers form three critical protein-protein interfaces with NusG-CTD, the β-subunit flap-tip of RNAP and the ω subunit (**Fig. 11B**).

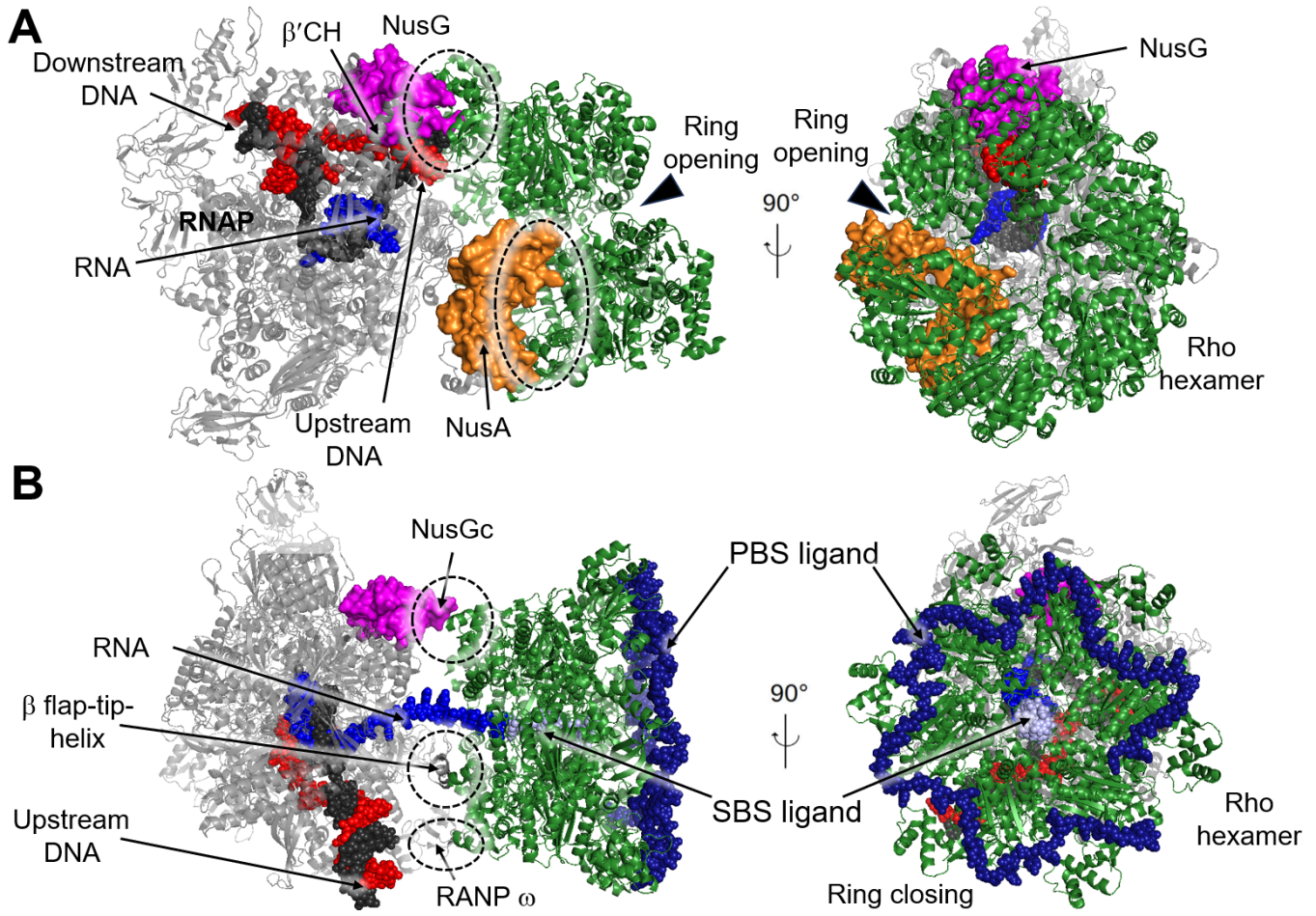

Fig. 11 A) Cryo-EM structure of *E. coli* Rho-dependent transcription pre-termination complex bound with NusG with Rho hexamer in open state (PDB 6XAV). **B)** *E. coli* Rho-dependent transcription pre-termination complex (PDB 8E6X and 8E6V) with Rho hexamer in closed state. Rho hexamer, NusG, NusA, tDNA, ntDNA, PBS ligand and SBS are colored forest green, magenta, orange, black, red, pale blue and density blue. Interfaces between Rho and RNAP, NusA or NusG are circled with dashed rings.

Mfd factor. Mfd, also known as transcription-repair coupling factor (TRCF), is a widely conserved bacterial protein links between DNA repair and transcription processes. Its major role is to recognize stalled RNAP at sites of DNA lesions. Once Mfd identifies the stalled RNAP, it recruits DNA excision repair machinery to the damaged site and promotes the dissociation of elongation complex [101]. Unlike Rho-dependent termination that involves RNA, Mfd functions as an ATP-dependent DNA translocase that binds to both DNA and RNAP simultaneously and consumes ATP to remove RNAP from the DNA template, clearing the transcriptional roadblock caused by DNA lesions and to facilitate efficient DNA repair [102]. Studies also reveal that Mfd contributes to the rapid development of antibiotic resistance in various bacterial species by augmenting mutation rates [103, 104]. This can be partially attributed to Mfd-dependent termination, which promotes mutagenic DNA repair through error-prone gap-filling mechanisms [105]. Therefore, Mfd may be a potential target for antimicrobial drug development to overcome antimicrobial resistance.

4. Development of bacterial transcription inhibitors

The structural studies of RNAP and its interactions with transcription factors provide abundant information for the structure-based drug design. We believe that the interdependent interactions between the RNAP core and transcription factors hold promise as targets for developing next-generation antibacterial agents, as these interactions are critical to gene expression. Moreover, confirmation of the "hotspots" through biological methods or theoretical calculations can accelerate the identification of PPI inhibitors, including those targeting bacterial transcription. In the following section, we would like to introduce some bacterial transcription inhibitors targeting PPI between RNAP and transcription factors.

4.1. Inhibitors of RNAP-σ factor interaction

Sigmacidins (C3 series). C3 (**1**) (**Fig. 12**) was discovered by *in silico* screen of a drug-like compound library [106]. Initial evaluation using a split-luciferase assay showed that C3 exhibited an IC_{50} of 6.40 ± 0.71 μM against the PPI between CH

and σ [107]. However, its antimicrobial activity against *Streptococcus pneumoniae* was moderate, with a minimum inhibitory concentration (MIC) of 256 μg/mL [107].

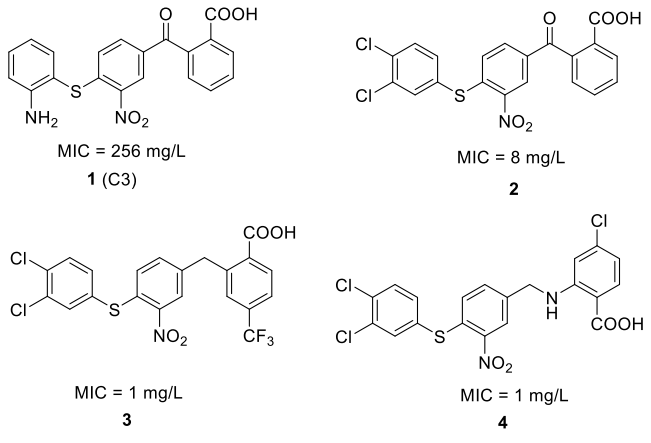

Fig. 12 Chemical structure of compound **1** and its derivatives (**2** to **4**) along with their activity against *S. pneumoniae*.

To enhance the antibacterial properties of C3, a comprehensive and systematic optimization strategy was employed, resulting in the synthesis of dozens of derivatives, such as compounds **2** to **4** [107-109] (**Fig. 11**). Compound **C3-005** (**2**), featuring 3,4-diCl substituents on the left benzene ring instead of the 2-NH_2, notably improved the antibacterial activity against *S. pneumoniae* with a MIC value of 8 μg/mL [107]. Strikingly, compound **3**, incorporating a benzyl benzoic acid moiety, demonstrated to be a up-and-coming antibacterial agent with a MIC value of low to 1 μg/mL [108]. Furthermore, compound **4**, characterized by an aminomethylene linker instead of a carbonyl linker, proved to be an efficient antimicrobial agent, with a MIC value of 1 μg/mL against *S. pneumoniae* and IC_{50} value of 6.8 ± 0.7 μM in disrupting the formation of RNAP holoenzyme. This compound also demonstrated time-dependent inhibition of bacterial growth and exerted inhibitory effects on bacterial central metabolism, suggesting its bacteriostatic effect with the reduced release of exotoxin [109]. Further sulfonamidyl derivatives of C3 also showed good antimicrobial activity [110]. The C3 series of compounds was coined sigmacidins to reflect the inhibitory function by mimicking σ factor and the benzoic acid structure [111].

C5 (DSHS00507). Compound **C5** (**5**) (**Fig. 13**) was discovered by an *in silico* screening of a drug-like compound library [106]. Notably, a refined pharmacophore model, which incorporated optimized conditions and was based on the PPI between $\sigma^A{}_{2.2}$ and β'CH region [112], was developed and utilized for comparison. The published article demonstrated that both compounds **1** and **5** showed about 80% inhibitory activity against RNAP holoenzyme formation by inhibiting *in vitro* β'CH-σ^A interaction at 500 μM, whereas compound **5** displayed inhibition activity even at lower concentrations. Moreover, an isothermal titration calorimetry (ITC) experiment confirmed that there were no interactions between compound **C5** and human Rpb1-CH, indicating its specific antibacterial activity. Meanwhile, antibacterial assays further corroborated the efficacy of compound C5, particularly against Gram-positive bacteria. For instance, the MIC value for *B. subtilis* was found to be ≤50 μM, while it was approximately 100 μM for community-acquired methicillin-resistant *Staphylococcus aureus* (CA-MRSA) [106].

GKL003. GKL003 (**6**) (**Fig. 14**), a bis-indole derivative, was discovered through a virtual screening approach targeting β'CH-$\sigma^A{}_{2.2}$ interaction [112, 113]. Experimental analysis using native gel electrophoresis revealed that GKL003 can inhibit RNAP

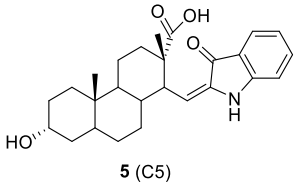

Fig. 13 Chemical structure of compound **5**.

holoenzyme formation *in vitro* by specifically targeting the PPI between $\sigma^A{}_{2.2}$ and β'CH region. Moreover, ITC experiments demonstrated that GKL003 specifically binds to the same region of β'CH that is required for interacting with $\sigma^A{}_{2.2}$, exhibiting a remarkable inhibition constant (K_i) value of approximately 0.6 nM. Further competition assays showed that GKL003 competitively inhibited the interaction between RNAP core and σ^A *in vitro*. Despite its excellent activity demonstrated *in vitro*, GKL003 exhibited limited efficacy against bacterial growth (≥1 mM), probably due to its poor ability to traverse bacterial membranes [112].

The optimization process of GKL003 led to the development of a bis-indole library, focusing on assessing their activity against the interaction between RNAP and σ^{70}/σ_A [114]. In order to develop smaller compounds with improved cell membrane penetration capabilities, the bis-indole scaffold was simplified into mono-indole or related benzofuran scaffolds, resulting in the synthesis of compounds **7** (GLK046) to **9** (**Fig. 14**). The obtained results showed that some of these derivatives exclusively inhibited *E. coli* and *B. subtilis* growth. However, the inhibitory rates of these compounds against β'CH-$\sigma_{2.2}$ interaction were relatively modest [115-118].

Anthranilic acid derivatives. Anthranilic acid derivatives (**10** to **12**) (**Fig. 15**) were identified as RNAP-σ^{70} inhibitors through virtual screening using a pharmacophore model based on a flexible alignment of several molecules with unknown or diverse binding sites on RNAP [119]. To assess their efficacy, an *in vitro* transcription assay was conducted, which revealed that compounds **10** to **12** possessed RNAP inhibition levels exceeding 20% at 200 μM. Subsequently, a series of derivatives were synthesized to explore the structure-activity relationship (SAR), resulting in the discovery of compound **13** as the most potent inhibitor. Further experiment demonstrated that compound **13** possessed the highest *in vitro* activity against the *E. coli* RNAP-σ interaction, with an IC_{50} value of 9 μM.

SB series compounds. Using a multiwell enzyme-linked immunosorbent assay (ELISA)-based approach, several small molecules (referred to as the "SB series") that inhibit the σ-RNAP interaction were discovered for the first time [120, 121]. Among these molecules, compound **14** (**Fig. 16**) demonstrated the ability to inhibit the binding of *E. coli* σ^{70} to RNAP, with an

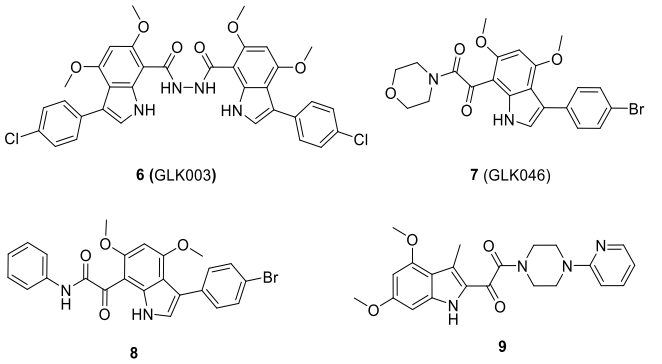

Fig. 15 Chemical structure of **6** (GLK003) and its derivatives **7** to **9** with mono-indole scaffold.

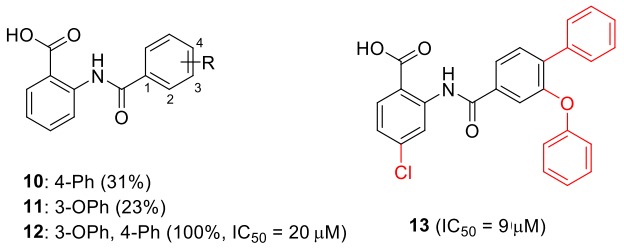

Fig. 14 Chemical structures of compound **9** to **13** and their *in vitro* activities against *E. coli* RNAP-σ interaction (IC_{50} value or percentage inhibition at 200 μM (SD <40%)).

IC_{50} value of 2 μM in the ELISA assay. Furthermore, compound **14** exhibited antibacterial effects against both Gram-positive and Gram-negative bacteria. For example, the MIC against *S. pneumoniae* was 2 μg/mL, against *Bacillus anthracis* was 0.1 μg/mL, and against *Bacteroides sp.* was 1 μg/mL. To explore the SAR of compound **14**, a comprehensive study was conducted, resulting in developing a series of phenyl-furanyl-rhodanines (PFRs) as antibacterial inhibitors of RNAP, including SB7 and SB8 [122]. SB7 (**15**) and SB8 (**16**) exhibited IC_{50} values of 3 and 1.8 μM, respectively, in inhibiting RNAP-σ interaction. Though the SB series compounds could block σ-RNAP interaction, their precise binding site remains unclear.

4.2. Inhibitors of NusB-NusE interactions

Nusbiarylins. Nusbiarylins represents a new class of antibacterial agents which specifically target bacterial rRNA synthesis. The nomenclature "nusbiarylins" was assigned to this series of compounds due to their interaction with the NusB protein and their distinctive biaryl structure [123]. The first

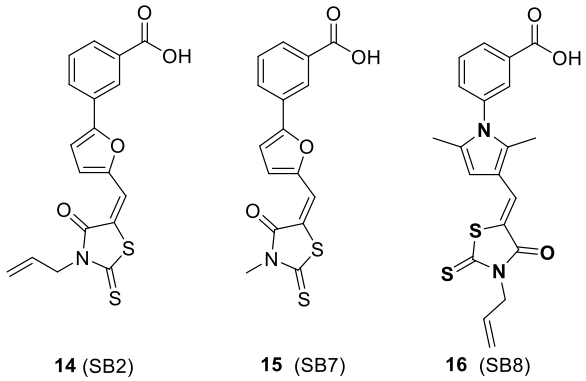

Fig. 17 Chemical structure of compounds **14** to **16**.

member of this class, MC4 (**17**) (**Fig. 17**), was discovered through an *in silico* screening approach utilizing a pharmacophore model previously described [124]. *In vitro* assays confirmed that MC4 effectively interrupted the NusB-NusE interaction, with an IC_{50} value of approximately 35 μM, and displayed a binding affinity to NusB with a dissociation constant (K_d) approximately 1.5 μM. In particular, MC4 exhibited significant growth inhibitory activity against a panel of *S. aureus* strains, with MIC as low as 8 μg/mL [125].

The SAR investigation of MC4 focused on the substitution of the benzyl rings and the bridge connecting them (**Fig. 17**) [123, 124, 126, 127]. Some of the derivatives (**18** to **22**) exhibited a dramatically

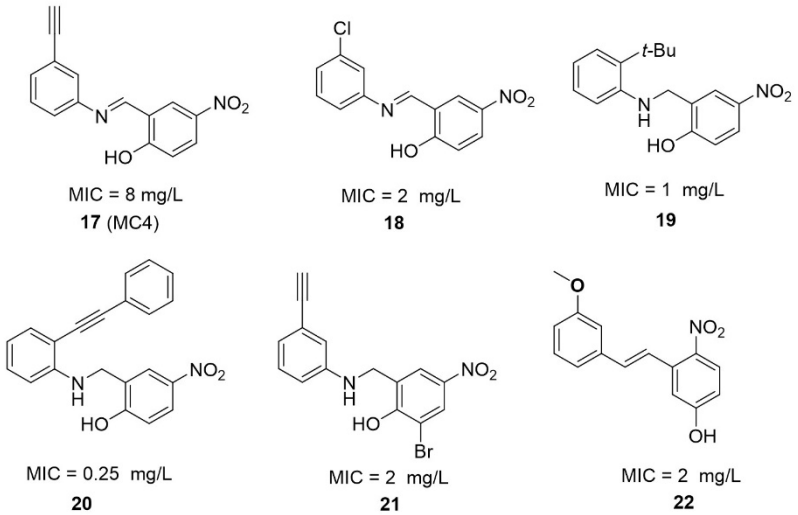

Fig. 16 SAR studies of MC4 and the structures of its derivatives. MIC values represent minimal inhibitory concentrations against *S. aureus*.

improved activity against a panel of pathogens, with MICs ranging from 0.25 to 2 μg/mL against methicillin- and vancomycin-resistant *S. aureus*, while demonstrating negligible cytotoxicity. However, the improvement in antibacterial efficacy was not very consistent with the NusB-NusE inhibitory action, which might be due to diverse cell membrane permeability.

Compounds 23 and 24. Compounds **23** and **24** (**Fig. 17**) were identified to be potent PPI inhibitors, with IC_{50} values of 6.1 μM and 19.8 μM, respectively in inhibiting NusB-NusE interaction. These compounds were discovered through an *in silico* screening of the mini-Maybridge compound library [128]. Further optimization of compound **24** resulted in the discovery of several derivatives with enhanced potency. Amongst, compound **25** showed 100% inhibition against both *B. subtilis* and *E. coli* at 200 μM [129].

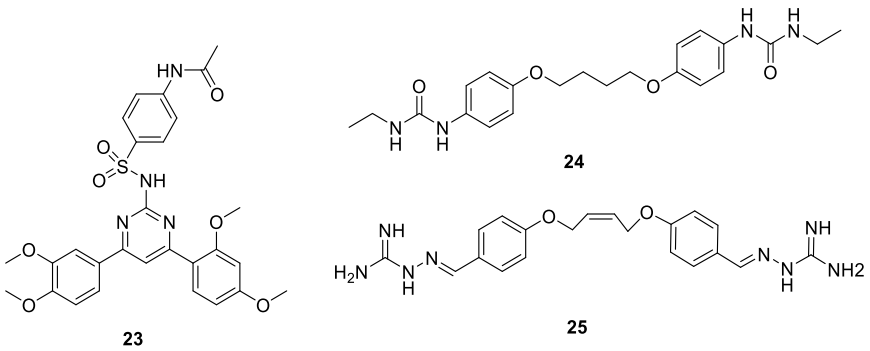

Fig. 18 Chemical structures of compounds **23** to **25**.

4.3. Inhibitors of Rho factor

Bicyclomycin. Bicyclomycin (**26**) is an antibiotic which was initially isolated from the culture filtrate of *Streptomyces sapporonensis* [130]. It exerts its antibacterial activity by binding to the secondary RNA binding (tracking) site on the Rho and hence affecting the poly(C)-dependent ATPase activity of the Rho factor in *E. coli*. This activity follows a non-competitive kinetic pattern concerning ATP [131, 132]. The extrapolated K_i for bicyclomycin was 2.8 μM in the presence of ribo$(C)_{10}$, whereas it increased to 26 μM in its absence [132].

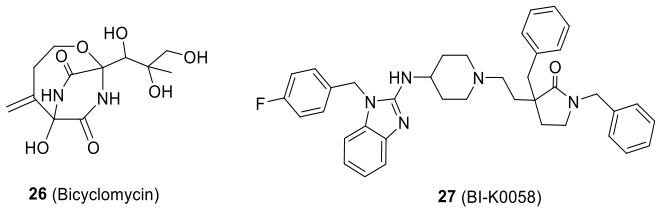

Fig. 19 Chemical structures of Bicylomycin and BI-K0058.

BI-K0058. BI-K0058 (**27**) was identified as an inhibitor of the poly(C)-dependent Rho-catalyzed hydrolysis of ATP through an *in vitro* ATPase assay on a chemical library containing 30,000 compounds. It effectively inhibits the ATPase activity of Rho with an IC_{50} of 25 μM. Additionally, BI-K0058 exhibited significant antimicrobial activity against two bacterial strains, *Neisseria gonorrhoeae* and *Moraxella catharralis*, with MICs ranging from 2.5 to 5 μM [133].

5. Discussion and conclusions

The continuing threat of multidrug resistance in bacterial infections, coupled with a lack of innovation in the discovery of new antimicrobial agents, underscores the pressing need for novel therapeutics. However, between 2010 and 2018, the Food and Drug Administration (FDA) only approved eight new antibacterial agents, which were all derived from established drug classes [134]. In 2019, the FDA approved Lefamulin, a first-in-class semi-synthetic pleuromutilin antibiotic with a unique mechanism of action. Lefamulin inhibits protein synthesis by binding to the peptidyl transferase center of the 50S bacterial ribosome, making it a viable treatment option for community-acquired bacterial pneumonia (CABP) in humans [134, 135]. However, the potential cost of Lefamulin may present a barrier to its widespread use, with intravenous treatment estimated at $205 and oral treatment at $275 per day [136]. Therefore, the search for new strategies to discover novel antibiotics remains both valuable and urgent.

This review has summarized the effectiveness and efficiency of targeting bacterial RNAP as a strategy for antibacterial therapy, exemplified by clinically utilized drugs, rifamycin and lipiarmycin. This innovative approach disrupts the formation of transcription complex and possess some advantages, in which it has potential to reduce the development of drug resistance. This is primarily because developing resistance to PPI inhibitors typically requires the occurrence of dual mutations, which incurs a higher energy cost.

Structural biology is critical in facilitating drug discovery by providing valuable insights into the three-dimensional structures of macromolecules and their interactions with corresponding partners. Over the past 20 years, a general framework of the structural basis for bacterial transcription cycles has been gradually revealed. By analyzing the interfaces between RNAP and its associated factors, critical domains or

hotspots have been identified, providing key clues for structure-based drug design.

Recently, there have been more and more outstanding research efforts towards the inhibition of bacterial transcriptional PPIs, especially some remarkable successes using *in silico* virtual screening techniques that utilize pharmacophore models constructed on the basis of the structural information. By screening or designing bioactive compounds with a known target, rapid modifications are allowed to enhance the selectivity of the compounds. However, it is worth noting that hit compounds with good activity on purified targets or bacteria may lose potency or become inactive after modifications. This can partially be attributed to the alternations in their interactions with the target or changes in permeability. Despite these challenges, targeting transcriptional PPIs remains a valid but underdeveloped strategy for antibiotic discovery.

Finally, the small molecular antibacterial agents described here are still at a preliminary stage of development and not yet considered clinical drugs. Though some of the most active compounds exhibit very low MIC values, they often require appropriate modifications to optimize their pharmacokinetic properties and enhance their drug-like characteristics, for instance, bioavailability, metabolic stability, and toxicity. Nevertheless, the comprehensive information outlined here serves as a useful foundation for the further development of next-generation antimicrobial agents targeting transcriptional PPIs. By building upon this knowledge and employing strategies to enhance the pharmacokinetic properties of these compounds, it is possible to pave the way for the eventual clinical translation of these promising agents into effective antibacterial therapies.

Conflicts of interest

The authors declare no conflict of interest.

Acknowledgements

We gratefully acknowledge the financial support from the Research Grants Council of the Hong Kong Special Administrative Region, China (PolyU 15100022 and C5008-19G to C.M., CUHK 14107919 to X.Y.), Hong Kong Polytechnic University (1-ZE2E and the State Key Laboratory of Chemical Biology and Drug Discovery to C.M.), Hong Kong Food and Health Bureau HMRF (19180052 to X.Y.) and the Chinese University of Hong Kong (Faculty of Medicine Faculty Innovation Award FIA2018/A/03, and Passion for Perfection Scheme PFP202210-008 to X.Y.), and Start-up Fund of Anhui Medical University (0601120201 to J.Y.).

References

1. M. A. Cook and G. D. Wright, *Science Translational Medicine*, 2022, **14,** eabo7793.
2. R. Aminov, *Biochemical Pharmacology*, 2017, **133**, 4-19.
3. T. M. Uddin, A. J. Chakraborty, A. Khusro, B. R. M. Zidan, S. Mitra, T. B. Emran, K. Dhama, M. K. H. Ripon, M. Gajdács, M. U. K. Sahibzada, M. J. Hossain and N. Koirala, *Journal of Infection and Public Health*, 2021, **14**, 1750-1766.
4. W. P. J. Smith, B. R. Wucher, C. D. Nadell and K. R. Foster, *Nature Reviews Microbiology*, 2023, **21**, 519-534.
5. P. G. Higgs and N. Lehman, *Nature Reviews Genetics*, 2015, **16**, 7-17.
6. X. Dai, S. Zhang and K. Zaleta-Rivera, *Molecular Biology Reports*, 2020, **47**, 1413-1434.
7. G. W. Li and X. S. Xie, *Nature*, 2011, **475**, 308-315.
8. A. Robinson and A. M. Van Oijen, *Nature Reviews Microbiology*, 2013, **11**, 303-315.
9. M. Wassenegger and G. Krczal, *Trends in Plant Science*, 2006, **11**, 142-151.
10. S. Spiegelman, A. Burny, M. R. Das, J. Keydar, J. Schlom, M. Travnicek and K. Watson, *Nature*, 1970, **227**, 563-567.
11. C. Ma, X. Yang and P. J. Lewis, *Microbiology and Molecular Biology Reviews*, 2016, **80**, 139-160.
12. P. Villain-Guillot, L. Bastide, M. Gualtieri and J. P. Leonetti, *Drug Discovery Today*, 2007, **12**, 200-208.
13. R. A. Adams, G. Leon, N. M. Miller, S. P. Reyes, C. H. Thantrong, A. M. Thokkadam, A. S. Lemma, D. M. Sivaloganathan, X. Wan and M. P. Brynildsen, *Journal of Antibiotics*, 2021, **74**, 786-798.
14. A. Venugopal and S. Johnson, *Clinical Infectious Diseases*, 2012, **54**, 568-574.
15. R. Kahan, D. J. Worm, G. V. De Castro, S. Ng and A. Barnard, *RSC Chemical Biology*, 2021, **2**, 387-409.
16. S. H. Kirsch, F. P. J. Haeckl and R. Müller, *Natural Product Reports*, 2022, **39**, 1226-1263.
17. F. Werner, *Molecular Microbiology*, 2007, **65**, 1395-1404.
18. F. Werner and D. Grohmann, *Nature Reviews Microbiology*, 2011, **9**, 85-98.
19. L. Delaye and A. Becerra, *Evolution: Education and Outreach*, 2012, **5**, 382-388.
20. M. L. Sokolova, I. Misovetc and K. V. Severinov, *Viruses*, 2020, **12,** 1064.
21. L. Minakhin, S. Bhagat, A. Brunning, E. A. Campbell, S. A. Darst, R. H. Ebright and K. Severinov, *Proceedings of the National Academy of Sciences of the United States of America*, 2001, **98**, 892-897.
22. J. Chen, H. Boyaci and E. A. Campbell, *Nature Reviews Microbiology*, 2021, **19**, 95-109.
23. F. Werner, *Chemical Reviews*, 2013, **113**, 8331-8349.
24. C. R. Woese, O. Kandler and M. L. Wheelis, *Proceedings of the National Academy of Sciences of the United States of America*, 1990, **87**, 4576-4579.
25. D. Grohmann and F. Werner, *Research in Microbiology*, 2011, **162**, 10-18.
26. K. S. Murakami, *Biomolecules*, 2015, **5**, 848-864.
27. G. Zhang, E. A. Campbell, L. Minakhin, C. Richter, K. Severinov and S. A. Darst, *Cell*, 1999, **98**, 811-824.
28. C. Sutherland and K. S. Murakami, *EcoSal Plus*, 2018, **8,** 10.1128/ecosalplus.ESP-0004-2018.
29. F. Werner, *Trends in Microbiology*, 2008, **16**, 247-250.

30. L. M. Iyer, E. V. Koonin and L. Aravind, *BMC Structural Biology*, 2003, **3**, 1-23.
31. S. Borukhov and E. Nudler, *Trends in Microbiology*, 2008, **16**, 126-134.
32. H. Mosaei and J. Harbottle, *Biochemical Society Transactions*, 2019, **47**, 339-350.
33. J. Pan, *Cancer Letters*, 2010, **292**, 149-152.
34. Y. Furuta, B. B. Gowen, K. Takahashi, K. Shiraki, D. F. Smee and D. L. Barnard, *Antiviral Research*, 2013, **100**, 446-454.
35. G. Muratore, L. Goracci, B. Mercorelli, A. Foeglein, P. Digard, G. Cruciani, G. Palù and A. Loregian, *Proceedings of the National Academy of Sciences of the United States of America*, 2012, **109**, 6247-6252.
36. S. I. Maffioli, Y. Zhang, D. Degen, T. Carzaniga, G. Del Gatto, S. Serina, P. Monciardini, C. Mazzetti, P. Guglierame, G. Candiani, A. I. Chiriac, G. Facchetti, P. Kaltofen, H. G. Sahl, G. Dehò, S. Donadio and R. H. Ebright, *Cell*, 2017, **169**, 1240-1248.
37. E. A. Campbell, N. Korzheva, A. Mustaev, K. Murakami, S. Nair, A. Goldfarb and S. A. Darst, *Cell*, 2001, **104**, 901-912.
38. A. Tupin, M. Gualtieri, F. Roquet-Banères, Z. Morichaud, K. Brodolin and J. P. Leonetti, *International Journal of Antimicrobial Agents*, 2010, **35**, 519-523.
39. M. Gualtieri, P. Villain-Guillot, J. Latouche, J. P. Leonetti and L. Bastide, *Antimicrobial Agents and Chemotherapy*, 2006, **50**, 401-402.
40. A. Tupin, M. Gualtieri, J. P. Leonetti and K. Brodolin, *EMBO Journal*, 2010, **29**, 2527-2537.
41. W. Lin, K. Das, D. Degen, A. Mazumder, D. Duchi, D. Wang, Y. W. Ebright, R. Y. Ebright, E. Sineva, M. Gigliotti, A. Srivastava, S. Mandal, Y. Jiang, Y. Liu, R. Yin, Z. Zhang, E. T. Eng, D. Thomas, S. Donadio, H. Zhang, C. Zhang, A. N. Kapanidis and R. H. Ebright, *Molecular Cell*, 2018, **70**, 60-71.
42. K. M. Herbert, W. J. Greenleaf and S. M. Block, *Annual Review of Biochemistry*, 2008, **77**, 149-176.
43. J. Griesenbeck, H. Tschochner and D. Grohmann, *Macromolecular Protein Complexes: Structure and Function*, **2017**, 225-270.
44. S. Borukhov, J. Lee and O. Laptenko, *Molecular Microbiology*, 2005, **55**, 1315-1324.
45. C. Mejía-Almonte, S. J. W. Busby, J. T. Wade, J. van Helden, A. P. Arkin, G. D. Stormo, K. Eilbeck, B. O. Palsson, J. E. Galagan and J. Collado-Vides, *Nature Reviews Genetics*, 2020, **21**, 699-714.
46. J. D. Helmann, *Molecular Microbiology*, 2019, **112**, 335-347.
47. A. Mazumder and A. N. Kapanidis, *Journal of Molecular Biology*, 2019, **431**, 3947-3959.
48. M. J. Kazmierczak, M. Wiedmann and K. J. Boor, *Microbiology and Molecular Biology Reviews*, 2005, **69**, 527-543.
49. D. G. Vassylyev, S. I. Sekine, S. Yokoyama and S. Yokoyama, *Nature*, 2002, **417**, 712-719.
50. M. S. B. Paget and J. D. Helmann, *Genome Biology*, 2003, **4,** 1-6.
51. K. S. Murakami and S. A. Darst, *Current Opinion in Structural Biology*, 2003, **13**, 31-39.
52. H. Fan, A. B. Conn, P. B. Williams, S. Diggs, J. Hahm, H. B. Gamper Jr, Y.-M. Hou, S. E. O'Leary, Y. Wang, G. M. Blaha, *Nucleic Acids Research*, 2017, **45**, 11043–11055.
53. A. Mustaev, J. Roberts and M. Gottesman, *Transcription*, 2017, **8**, 150-161.
54. G. A. Belogurov and I. Artsimovitch, *Journal of molecular biology*, 2019, **431**, 3975-4006.
55. J. Y. Kang, T. V. Mishanina, R. Landick and S. A. Darst, *Journal of molecular biology*, 2019, **431**, 4007-4029.
56. T. Jayasinghe, Z. F. Mandell, A. V. Yakhnin, M. Kashlev and P. Babitzke, *Journal of bacteriology*, 2022, **204**, e00534-21.
57. K. Liu, Y. Zhang, K. Severinov, A. Das and M. M. Hanna, *EMBO Journal*, 1996, **15**, 150-161.
58. B. Gopal, L. F. Haire, S. J. Gamblin, E. J. Dodson, A. N. Lane, K. G. Papavinasasundaram, M. J. Colston and G. Dodson, *Journal of Molecular Biology*, 2001, **314**, 1087-1095.
59. K. Schweimer, S. Prasch, P. S. Sujatha, M. Bubunenko, M. E. Gottesman and P. Rösch, *Structure*, 2011, **19**, 945-954.
60. X. Guo, A. G. Myasnikov, J. Chen, C. Crucifix, G. Papai, M. Takacs, P. Schultz and A. Weixlbaumer, *Molecular Cell*, 2018, **69**, 816-827.
61. X. Yang, S. Molimau, G. P. Doherty, E. B. Johnston, J. Marles-Wright, R. Rothnagel, B. Hankamer, R. J. Lewis and P. J. Lewis, *EMBO Reports*, 2009, **10**, 997-1002.
62. C. Ma, M. Mobli, X. Yang, A. N. Keller, G. F. King and P. J. Lewis, *Nucleic Acids Research*, 2015, **43**, 2829-2840.
63. A. V. Yakhnin, M. Kashlev and P. Babitzke, *Critical reviews in biochemistry and molecular biology*, 2020, **55**, 716-728.
64. E. Burova, S. C. Hung, V. Sagitov, B. L. Stitt and M. E. Gottesman, *Journal of Bacteriology*, 1995, **177**, 1388-1392.
65. K. M. Herbert, J. Zhou, R. A. Mooney, A. La Porta, R. Landick and S. M. Block, *Journal of molecular biology*, 2010, **399**, 17-30.
66. A. V. Yakhnin, H. Yakhnin and P. Babitzke, *Proceedings of the National Academy of Sciences*, 2008, **105**, 16131-16136.
67. B. Liu and T. A. Steitz, *Nucleic Acids Research*, 2017, **45**, 968-974.
68. A. V. Yakhnin, P. C. FitzGerald, C. McIntosh, H. Yakhnin, M. Kireeva, J. Turek-Herman, Z. F. Mandell, M. Kashlev and P. Babitzke, *Proceedings of the National Academy of Sciences*, 2020, **117**, 21628-21636.
69. R. K. Vishwakarma, M. Z. Qayyum, P. Babitzke and K. S. Murakami, *Proceedings of the National Academy of Sciences*, 2023, **120**, e2218516120.
70. D. L. Court, T. A. Patterson, T. Baker, N. Costantino, X. Mao and D. I. Friedman, *Journal of Bacteriology*, 1995, **177**, 2589-2591.
71. J. R. Stagno, A. S. Altieri, M. Bubunenko, S. G. Tarasov, J. Li, D. L. Court, R. A. Byrd and X. Ji, *Nucleic Acids Research*, 2011, **39**, 7803-7815.
72. A. S. Altieri, M. J. Mazzulla, D. A. Horita, R. H. Coats, P. T. Wingfield, A. Das, D. L. Court and R. A. Byrd, *Nature Structural Biology*, 2000, **7**, 470-474.
73. B. Gopal, L. F. Haire, R. A. Cox, M. J. Colston, S. Major, J. A. Brannigan, S. J. Smerdon and G. Dodson, *Nature Structural Biology*, 2000, **7**, 475-478.

74. J. J. C. S. H. M. A. Greenblatt, 1992, **22**, 203-226.
75. B. T. Wimberly, D. E. Brodersen, W. M. Clemons Jr, R. J. Morgan-Warren, A. P. Carter, C. Vonrheln, T. Hartsch and V. Ramakrishnan, *Nature*, 2000, **407**, 327-339.
76. X. Luo, H. H. Hsiao, M. Bubunenko, G. Weber, D. L. Court, M. E. Gottesman, H. Urlaub and M. C. Wahl, *Molecular Cell*, 2008, **32**, 791-802.
77. R. Das, S. Loss, J. Li, D. S. Waugh, S. Tarasov, P. T. Wingfield, R. A. Byrd and A. S. Altieri, *Journal of Molecular Biology*, 2008, **376**, 705-720.
78. J. Drögemüller, M. Strauß, K. Schweimer, M. Jurk, P. Rösch and S. H. Knauer, *Scientific reports*, 2015, **5**, 16428.
79. B. M. Burmann, K. Schweimer, X. Luo, M. C. Wahl, B. L. Stitt, M. E. Gottesman and P. Rösch, *Science*, 2010, **328**, 501-504.
80. M. T. Marr and J. W. Roberts, *Molecular cell*, 2000, **6**, 1275-1285.
81. A. Lass-Napiorkowska and T. Heyduk, *Biochemistry*, 2016, **55**, 647-658.
82. F. Toulmé, C. Mosrin-Huaman, J. Sparkowski, A. Das, M. Leng and A. R. Rahmouni, *The EMBO journal*, 2000, **19**, 6853-6859.
83. T. Fouqueau, M. E. Zeller, A. C. Cheung, P. Cramer and M. Thomm, *Nucleic acids research*, 2013, **41**, 7048-7059.
84. C. Saint-André, M. Takacs, G. Papai, C. Crucifix, X. Guo, J. Ortiz and A. Weixlbaumer, *Molecular cell*, 2019, **75**, 298-309.
85. D. Koulich, M. Orlova, A. Malhotra, A. Sali, S. A. Darst and S. Borukhov, *Journal of Biological Chemistry*, 1997, **272**, 7201-7210.
86. R. N. Fish and C. M. Kane, *Biochimica et Biophysica Acta (BBA)-Gene Structure and Expression*, 2002, **1577**, 287-307.
87. N. Opalka, M. Chlenov, P. Chacon, W. J. Rice, W. Wriggers and S. A. Darst, *Cell*, 2003, **114**, 335-345.
88. M. N. Vassylyeva, V. Svetlov, A. D. Dearborn, S. Klyuyev, I. Artsimovitch and D. G. Vassylyev, *EMBO reports*, 2007, **8**, 1038-1043.
89. N. Loizos and S. A. Darst, *Journal of Biological Chemistry*, 1999, **274**, 23378-23386.
90. A. Ray-Soni, M. J. Bellecourt and R. Landick, *Annual review of biochemistry*, 2016, **85**, 319-347.
91. L. You, E. O. Omollo, C. Yu, R. A. Mooney, J. Shi, L. Shen, X. Wu, A. Wen, D. He and Y. Zeng, *Nature*, 2023, **613**, 783-789.
92. P. Mitra, G. Ghosh, M. Hafeezunnisa and R. Sen, *Annual review of microbiology*, 2017, **71**, 687-709.
93. J. W. Roberts, *Journal of molecular biology*, 2019, **431**, 4030-4039.
94. H. Kohn and W. Widger, *Current Drug Targets - Infectious Disorders*, 2005, **5**, 273-295.
95. C. Zhu, X. Guo, P. Dumas, M. Takacs, M. m. Abdelkareem, A. Vanden Broeck, C. Saint-André, G. Papai, C. Crucifix and J. Ortiz, *Nature Communications*, 2022, **13**, 1546.
96. J. M. Peters, R. A. Mooney, J. A. Grass, E. D. Jessen, F. Tran and R. Landick, *Genes and Development*, 2012, **26**, 2621-2633.
97. M. R. Lawson, W. Ma, M. J. Bellecourt, I. Artsimovitch, A. Martin, R. Landick, K. Schulten and J. M. Berger, *Molecular Cell*, 2018, **71**, 911-922.
98. N. Said, T. Hilal, N. D. Sunday, A. Khatri, J. Bürger, T. Mielke, G. A. Belogurov, B. Loll, R. Sen and I. Artsimovitch, *Science*, 2021, **371**, eabd1673.
99. Z. Hao, V. Epshtein, K. H. Kim, S. Proshkin, V. Svetlov, V. Kamarthapu, B. Bharati, A. Mironov, T. Walz and E. Nudler, *Molecular cell*, 2021, **81**, 281-292. e288.
100. V. Molodtsov, C. Wang, E. Firlar, J. T. Kaelber and R. H. Ebright, *Nature*, 2023, **614**, 367-374.
101. J. Roberts and J.-S. Park, *Current opinion in microbiology*, 2004, **7**, 120-125.
102. A. J. Smith, C. Pernstich and N. J. Savery, *Nucleic acids research*, 2012, **40**, 10408-10416.
103. J. Han, O. Sahin, Y.-W. Barton and Q. Zhang, *PLoS pathogens*, 2008, **4**, e1000083.
104. M. N. Ragheb, M. K. Thomason, C. Hsu, P. Nugent, J. Gage, A. N. Samadpour, A. Kariisa, C. N. Merrikh, S. I. Miller and D. R. Sherman, *Molecular cell*, 2019, **73**, 157-165.
105. H. C. Leyva-Sánchez, N. Villegas-Negrete, K. Abundiz-Yañez, R. E. Yasbin, E. A. Robleto and M. Pedraza-Reyes, *Journal of Bacteriology*, 2020, **202**, e00807-19.
106. C. Ma, X. Yang and P. J. Lewis, *ACS Infectious Diseases*, 2016, **2**, 39-46.
107. J. Ye, A. J. Chu, L. Lin, X. Yang and C. Ma, *Molecules*, 2019, **24,** 2902.
108. J. Ye, A. J. Chu, L. Lin, S. T. Chan, R. Harper, M. Xiao, I. Artsimovitch, Z. Zuo, C. Ma and X. Yang, *European Journal of Medicinal Chemistry*, 2020, **208,** 112671.
109. J. Ye, A. J. Chu, R. Harper, S. T. Chan, T. L. Shek, Y. Zhang, M. Ip, M. Sambir, I. Artsimovitch, Z. Zuo, X. Yang and C. Ma, *Journal of Medicinal Chemistry*, 2020, **63**, 7695-7720.
110. J. Ye, C. H. Kan, Y. Zheng, T. F. Tsang, A. J. Chu, K. H. Chan, X. Yang, C. Ma, *Bioorganic Chemistry*, 2024, **143**, 106983.
111. J. Ye, X. Yang, C. Ma, *International Journal of Molecular Sciences*, 2022, **23**, 4085.
112. C. Ma, X. Yang, H. Kandemir, M. Mielczarek, E. B. Johnston, R. Griffith, N. Kumar and P. J. Lewis, *ACS Chemical Biology*, 2013, **8**, 1972-1980.
113. E. B. Johnston, P. J. Lewis and R. Griffith, *Protein Science*, 2009, **18**, 2287-2297.
114. M. Mielczarek, R. V. Devakaram, C. Ma, X. Yang, H. Kandemir, B. Purwono, D. S. Black, R. Griffith, P. J. Lewis and N. Kumar, *Organic & Biomolecular Chemistry*, 2014, **12**, 2882-2894.
115. M. Mielczarek, R. V. Thomas, C. Ma, H. Kandemir, X. Yang, M. Bhadbhade, D. S. Black, R. Griffith, P. J. Lewis and N. Kumar, *Bioorganic & medicinal chemistry*, 2015, **23**, 1763-1775.
116. O. Thach, M. Mielczarek, C. Ma, S. K. Kutty, X. Yang, D. S. Black, R. Griffith, P. J. Lewis and N. Kumar, *Bioorganic & Medicinal Chemistry*, 2016, **24**, 1171-1182.
117. D. S. Wenholz, M. Zeng, C. Ma, M. Mielczarek, X. Yang, M. Bhadbhade, D. S. C. Black, P. J. Lewis, R. Griffith and N. Kumar, *Bioorganic & medicinal chemistry letters*, 2017, **27**, 4302-4308.
118. D. S. Wenholz, M. Miller, C. Dawson, M. Bhadbhade, D. S. Black, R. Griffith, H. Dinh, A. Cain, P. Lewis and N. Kumar, *Bioorganic Chemistry*, 2022, **118**, 105481.

119. S. Hinsberger, K. Hüsecken, M. Groh, M. Negri, J. Haupenthal and R. W. Hartmann, *Journal of Medicinal Chemistry*, 2013, **56**, 8332-8338.
120. E. André, L. Bastide, P. Villain-Guillot, J. Latouche, J. Rouby and J. P. Leonetti, *Assay and Drug Development Technologies*, 2004, **2**, 629-635.
121. E. André, L. Bastide, S. Michaux-Charachon, A. Gouby, P. Villain-Guillot, J. Latouche, A. Bouchet, M. Gualtiéri and J. P. Leonetti, *Journal of Antimicrobial Chemotherapy*, 2006, **57**, 245-251.
122. P. Villain-Guillot, M. Gualtieri, L. Bastide, F. Roquet, J. Martinez, M. Amblard, M. Pugniere and J. P. Leonetti, *Journal of Medicinal Chemistry*, 2007, **50**, 4195-4204.
123. J. Ye, X. Yang, C. Ma, *International Journal of Molecular Sciences*, 2022, **24**, 339.
124. Y. Qiu, S. T. Chan, L. Lin, T. L. Shek, T. F. Tsang, Y. Zhang, M. Ip, P. K. S. Chan, N. Blanchard, G. Hanquet, Z. Zuo, X. Yang and C. Ma, *Bioorganic Chemistry*, 2019, **92,** 103203.
125. X. Yang, M. J. Luo, A. C. Yeung, P. J. Lewis, P. K. Chan, M. Ip and C. Ma, *Biochemistry*, 2017, **56**, 5049-5052.
126. Y. Qiu, S. T. Chan, L. Lin, T. L. Shek, T. F. Tsang, N. Barua, Y. Zhang, M. Ip, P. K. S. Chan, N. Blanchard, G. Hanquet, Z. Zuo, X. Yang and C. Ma, *European Journal of Medicinal Chemistry*, 2019, **178**, 214-231.
127. Y. Qiu, A. J. Chu, T. F. Tsang, Y. Zheng, N. M. Lam, K. S. L. Li, M. Ip, X. Yang and C. Ma, *Bioorganic Chemistry*, 2022, **124**, 105863.
128. P. J. Cossar, C. Ma, C. P. Gordon, J. I. Ambrus, P. J. Lewis and A. McCluskey, *Bioorganic and Medicinal Chemistry Letters*, 2017, **27**, 162-167.
129. P. J. Cossar, M. K. Abdel-Hamid, C. Ma, J. A. Sakoff, T. N. Trinh, C. P. Gordon, P. J. Lewis and A. McCluskey, *ACS Omega*, 2017, **2**, 3839-3857.
130. T. Miyoshi, N. MIYAIRI, H. AOKI, M. KOHSAKA, H.-I. SAKAI and H. IMANAKA, *The Journal of antibiotics*, 1972, **25**, 569-575.
131. A. Zwiefka, H. Kohn and W. R. Widger, *Biochemistry*, 1993, **32**, 3564-3570.
132. A. Magyar, X. Zhang, H. Kohn and W. R. Widger, *Journal of Biological Chemistry*, 1996, **271**, 25369-25374.
133. L. Carrano, P. Alifano, E. Corti, C. Bucci and S. Donadio, *Biochemical and biophysical research communications*, 2003, **302**, 219-225.
134. M. P. Veve and J. L. Wagner, *Pharmacotherapy*, 2018, **38**, 935-946.
135. Y. R. Lee and K. L. Jacobs, *Drugs*, 2019, **79**, 1867-1876.
136. P. N. Malani, *JAMA*, 2019, **322**, 1671-1672.